Proceedings of the Twenty-first (2011) International Offshore and Polar Engineering Conference
Maui, Hawaii, USA, June 19-24, 2011

ISBN 978-1-880653-96-8 (Set); ISSN 1098-6189 (Set); www.isope.org

Seasonal Simulations of a Coupled Ice-ocean Model in the Bohai Sea and North Yellow Sea since the Winter of 1997/1998

Yu Liu[1,2] Qinzheng Liu[2] Jie Su[1] Maoning Tang[2] Shan Bai[2]
(1)College of Physical and Environmental Oceanography, Ocean University of China, Qingdao, China
(2) Key Laboratory of Research on Marine Hazards Forecasting, National Marine Environmental Forecasting Center, Beijing, China

ABSTRACT

A fine-resolution coupled ice-ocean model configured for the Bohai Sea and North Yellow Sea is presented. A horizontal grid spacing of 3.7km×2.8km was used in this coupled model. Seasonal simulations were made from the winters of 1997/1998 to 2008/2009. By comparing of the simulation results and the remote sensing images, the ice-ocean coupled model reasonably reproduces the seasonal variations of the sea ice conditions in the Bohai Sea and North Yellow Sea. The predicted ice-freezing date, ice-ending date and ice periods are in fairly good agreement with observations, and some are even identical to measurements. Moreover, the simulation of maximum sea ice extent date matches well. Normally, the sea ice thickness of the west part in Liaodong bay is less than that of the east part, which can be reproduced well by the ice-ocean coupled model. However, during the melting period, simulated sea ice melts much faster than observations, and the model loses accuracy in simulation of specific ice thickness distribution.

KEY WORDS: Coupled Ice-ocean Model; the Bohai Sea and North Yellow Sea; Sea Ice Concentration; Sea Ice Extent; Sea Ice Period; Sea Ice Thickness; Seasonal Variations.

INTRODUCTION

The Bohai Sea and North Yellow Sea are the only regions with sea ice in China Seas, and are almost the lowest-latitude regions ($37^\circ - 41^\circ N$, $117.5^\circ - 127^\circ E$, see Fig.1) which ice can naturally form in the world. Every winter, sea ice in these areas imposes different impacts on shipping, offshore oil and gas exploration, with oil platform collapsed, ships damaged, shipping stopped during severe ice conditions in history. The heaviest sea ice disaster took place in the winter of 1969, one of the three oil platforms was pushed down by drifting ice and another was damaged severely in the Bohai Sea. There were 8 ships stranded, 19 ships frozen on the sea and 5 huge ships of a million ton were broken by pack ice (Zhang, 1986; Bai et al., 1998). Even during the years of mild ice condition, there are also disasters at parts of the Bohai Sea, such as in the 2007 winter (Zhang, 2007). Therefore, sea ice is one major factor to be considered for marine engineering design, shipping and exploration for the ocean environment in the Bohai Sea and North Yellow Sea.

Since 1980s', by using field observation and experimentation, data analysis and numerical simulation, a series of studies on sea ice dynamics and thermodynamics have been carried out in China. The air-ice and air-sea heat budgets were calculated by using observed data at platforms and other field data (Wang et al., 1982). Sea ice thermodynamic processes were discussed, including solar radiation penetration through ice, the "thermal reservoir" effect of brine pocket and the processes which determine sea ice formation and growth, such as heat conduction among ice and thermal forces of atmosphere and ocean (Wu et al., 1992). Based on research of these sea ice thermal processes, parameterizations of sea ice thermal processes were proposed to determine the sea ice thermal growth function (Wu, 1991; Wang et al., 1994). According to non-uniformity caused by ice breaking and ice ridging, deformation functions was introduced, sea ice dynamic models was developed, and numerical experiments of ice drift was taken in the Bohai Sea (Wang, et al., 1984; 1994, Wu, et al., 1995; 1998). By using the open water, level ice and ridged ice to depict sea ice distribution within one grid, a dynamic-thermodynamic sea ice model was developed in the Bohai Sea, and has been applied to operational ice numerical forecast in NMEFC (National Marine Environmental Forecasting Center), China (Yang et al., 1991 and Bai et al., 1998).

Based on research of the interactions between atmosphere, ice and ocean, the ice–ocean coupled model has both scientific significance and practical value in terms of long-term study of sea ice or even climate change in this area. The establishment of global and North Pacific ocean-atmosphere coupled climate system has been used for short-term climate prediction (Zhang et al., 2000; Liu et al., 2000, 2004).

Over the past years, the numerical sea ice model research focused on the sea ice simulation and forecasting application in the Bohai Sea in China. Gradually, the regional ice-ocean coupled model has been developed. An ice-ocean coupled model was developed by using POM and a viscous - plastic thermodynamic-dynamic sea ice model in the Bohai Sea, and continuous sea ice simulations for two representative winters were taken, which got encouraging results(Su et al., 2004；2005).

All the previous calculation domains of regional sea ice models or ice-ocean coupled models were limited to the Bohai Sea in China. However, the Bohai Sea and the Yellow Sea are closely linked, and the sea ice occurrence and disappearance in North Yellow Sea is closely related to the marine environment of the Bohai Sea, thus may in some way affect

the sea ice occurrence and disappearance in the Bohai Sea. So in this paper, based on the Arctic ice-ocean coupled model (Wang, 2005) and some improvements including model's parameter optimization, the shallow water treatment and open boundary treatment, a coupled ice-ocean model suitable for the Bohai Sea and North Yellow Sea with a broad shallow water area was developed, which has more difficulty in open boundary treatment than previous domain. In addition, all previous simulation periods of regional ice-ocean coupled models were no more than 2 winters in China. In this paper, by using this ice-ocean coupled model and the regional atmospheric reanalysis data, a series of seasonal evolutions of sea ice cover have been simulated and analyzed from the winters of 1997/1998 to 2008/2009 in the Bohai Sea and North Yellow Sea.

1. A brief description of the ice-ocean coupled model

According to the specific features of sea ice in the Bohai Sea and North Yellow Sea, a coupled ice-ocean model was developed based on the three-dimensional Princeton Ocean Model (POM) and the thermodynamic-dynamic sea ice model.

1.1 Ice model in the ice-ocean coupled system

The Sea ice model includes a multi-category ice thermodynamic model based on ice thickness distribution function (Throndike et al., 1975; Hibler, 1980) and a dynamic sea ice model based on viscous-plastic constitutive law (Hibler, 1979).

Ice thickness equation satisfies continuity equation:

$$\frac{\partial g}{\partial t}+\nabla\cdot(u_i g)=-\frac{\partial[f(h)g]}{\partial h}+R(h,g,u_i) \tag{1}$$

where, g is the probability density of sea ice thickness distribution, $g(h)dh$ is fractional area covered by ice in the thickness range $(h,h+dh)$ in a grid. Therefore, the average ice thickness $\bar{h}$ and ice concentration A can be expressed by $g(h)$,

$$A=\int_{0+}^{h} g(h)dh \tag{2}$$

$$\bar{h}=\int_{0}^{h} g(h)hdh \tag{3}$$

where, u_i is the horizontal ice velocity, $f(h)$ is the rate of thermodynamic ice growth in vertical direction which is determined by the flux of air-ice interfaces, ice-water flux on the bottom of the ice, and thermodynamic process within the sea ice. The main thermodynamic process is shown in Figure 2.

$R(h,g,u_i)$ is dynamic ridging redistribution function of sea ice, which is the parameterization based on the dynamic process of the open water formation and ice ridging. This parameterization is employed to ensure the ice volume conservation during sea ice deformation process. In this paper Yao's parameterization method (2000) was used.

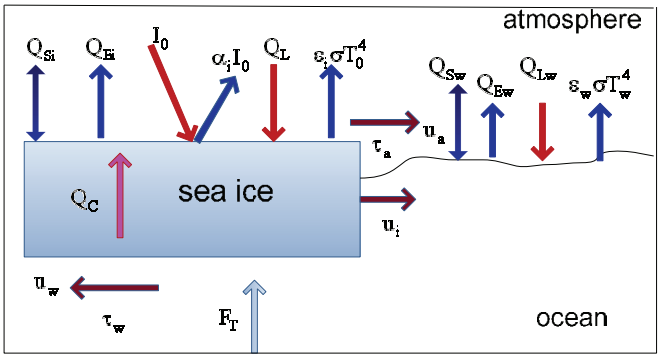

Fig.2 sketch map of the air-ice-ocean interaction

Dynamic sea ice model is used for solving the ice velocity u_i。It is calculated by the momentum equation.

$$m\frac{d}{dt}u_i+m\hat{f}\times u_i=-mg\nabla H+A(\tau_a-\tau_w)+\nabla\cdot\sigma \tag{4}$$

where $\hat{f}$ is Coriolis parameter, m is sea ice mass, ∇H is gradient of sea surface tilt, A is the ice concentration, τ_a and τ_w are the momentum fluxes in air-ice interface and ice-water interface separately, called wind stress and ice water interface stress as well. They are calculated by parametric formulae:

$$\tau_a=\rho_a C_{ai}|u_a|u_a \tag{5}$$

$$\tau_{wi}/\rho_w=\frac{ku_*}{\ln(z/z_0)}(u_i-u_w) \tag{6}$$

where u_a is wind velocity; u_w is velocity of top layer of water, u_i is sea ice drift velocity, C_{ai} is bulk coefficient which is set to 2.3×10-3 here; ρ_a and ρ_w are air and water density respectively, σ is internal ice stress tensor which is determined by the viscous-plastic constitutive law of sea ice (Hibler, 1979) . Viscous-plastic rheology is an effective method for simulating sea ice with strongly nonlinear dynamics process. It can overcome the problem caused by elastic waves in the elastic-plastic rheology (Colony and Rothrock, 1980), and can conveniently derive differential equations on fixed Euler grids. By using implicit scheme, time step can be larger without losing stability. This is advantageous in simulating sea ice long-term changes, such as seasonal variation. It is more suitable for the study of the sea ice properties in the ice margin zone.

1.2 Ocean model in the ice-ocean coupled system

The ocean model is based on the three-dimensional Princeton Ocean Model (POM). The model has been widely used. It can be used not only to simulate the estuaries, coastal areas, but also to simulate the large scale ocean. The model is a free surface, vertically sigma coordinate ocean model with an imbedded second moment turbulence closure sub-model to provide vertical mixing coefficients. Smagorinsky diffusivity scheme is applied for horizontal diffusion along sigma surfaces. A split time step of internal and external mode is used in time integration. The model is especially appropriate for the three-dimensional numerical simulation of ocean near shore.

Physically speak, for each grid of the model domain, the thickness of the water column must satisfy the physical constraints of not less than 0, but the results of POM model cannot guarantee to satisfy $h+\eta\geq 0$ automatically (where h is the average water depth, η is the water surface elevation relative to mean sea level, $h+\eta$ is water column thickness). Since both of Bohai Sea and Yellow Sea have a large intertidal zone, a corresponding treatment has been added to ensure $h+\eta<0$. This has improved the model performance. Also, boundary treatment is identical to the previous version of POM, but wave speed in the radiation boundary condition was represented by diagnosed group wave speed (Liu et al.，2005).

1.3 The parameterization of the physics in ice-ocean interface

The heat and salt fluxes in ice-ocean interface are determined by boundary layer process of the ocean mixed layer under ice. Mellor and Kantha (1989) have discussed in details the mixing process under the ice layer and its parameterization. In grids with ice, the ocean heat flux under ice layer is calculated by using the bulk parameterization formula as:

$$F_T=-\rho_w C_p C_{Tz}(T_f-T) \tag{7}$$

where C_p is specific heat of water; T is the sea water temperature of the top model layer; heat transfer coefficient C_{Tz} is determined by equation (8)

$$C_{Tz} = \frac{u_*}{P_{rt}\ln(-z/z_0)/k + B_T} \tag{8}$$

$$B_T = b(z_0 u_*/\nu)^{1/2} P_r^{2/3} \tag{9}$$

where, u_* is friction velocity; P_{rt} is turbulent Prandtl number; z is the depth of model's top layer; z_0 is roughness coefficient for the ice-water interface; k is Von Karman constant; B_T is molecular sub-layer correction in ice-water interface based on the law of the wall. It is determined by the molecular Prandtl number. The molecular sub-layer correction is represented by where P_r is a molecular Prandtl number, ν is the kinematic viscosity coefficient; b is the empirical constants set to 3.

In the sea ice covered grid, there is a flux of salt into the ocean while freezing, and a (negative) flux when sea water is melting. Net effect of precipitation and evaporation can also change water salinity. The total salt flux is parameterized as equation (10).

$$F_S = (W_{AI} + W_{IW} + W_{AW})(S_I - S) + (1-A)S(P-E) \tag{10}$$

where, S_I is the salinity of sea ice, and it is unified to 5psu in the model; S is sea water salinity of the model top layer, $(P-E)$ is the difference between precipitation and evaporation.

Stress τ_{wi} in ice-water interface is calculated by the bulk formula (11)

$$\tau_{wi}/\rho_w = \frac{k u_*}{\ln(z/z_0)}(u_i - u_w) \tag{11}$$

where, u_w is the sea water velocity of the top layer of the model; u_i is the sea ice drift velocity.

2. The model configuration

The compuational domain is 117°30′～127°00′E, 37°～41°N. The spatial resolution is 2′×2′ degree (3.7km×2.8km) in latitude and longitude direction for both sea ice model and ocean model. The total grid number is 34606 with 286 in the x direction and 121 in the y direction. Arakawa-C grid is used in ocean model. The vertical layer is set to 11 levels. The integral time step is 20s for the external mode and 600s for the internal mode. To consider the logarithmic profile distribution of the upper and bottom boundary layers, the 11 σ layers are (0.0, -0.018, -0.036, -0.071, -0.143, -0.286, -0.429, -0.571, -0.714, -0.857, -1.0). Arakawa-B grid is used in sea ice model. The integration time step is 600s. For the models that use multi-category ice thickness distribution function, the classifications based on sea ice thickness have some influence on the model results. Identification of thin ice is important for the air-water heat exchange and feedback process. In the Bohai Sea and North Yellow Sea, sea ice is first-year ice and is much thinner than that in polar region. The thickness of level ice here is generally 5cm to 50cm, and even for the coastal area thickness of level ice rarely exceeds 1m. In the northern part of Liaodong Bay with most serious sea ice piling up, the height of ridged ice can be 2.0m to 3.0m, with the maximum ridge ice thickness sometimes up to 6m. Considering the reliability and computational efficiency of the simulation, the model is set to 12 categories ice thickness, the thickness category scheme is shown in Table 1.

Table.1 Categories of the sea ice thickness

n	1	2	3	4	5	6
Thickness (cm)	0	0-2	2-5	5-10	10-15	15-20

n	7	8	9	10	11	12
Thickness (cm)	20-25	25-30	30-40	40-50	50-75	>75

The initial fields of temperature and salinity use climatologically 3-dimensional temperature and salinity analysis fields based on hydrology Atlas of the Bohai Sea and Yellow Sea (1993). Sea water temperature fields of all layers are corrected empirically according to historical sea surface temperature data from NMEFC.

Surface atmospheric forcing fields of ice-ocean coupled model are obtained from regional marine meteorological reanalysis data of the NMEFC, including hourly air temperatures, air humidity at 2 meters, wind speed and direction at 10 meter height above sea surface, with spatial resolution of 10km×10km. The meteorological forcing field is obtained by linear interpolated at each time step.

Synchronous coupled calculation scheme is adopted in ice-ocean coupled model of the Bohai Sea and North Yellow Sea. At each time step, the coupler first diagnostically calculates the fluxes of heat, momentum, and salinity in air-ice-sea interface based on the model variables of atmosphere, ocean and sea ice. Then these fluxes are passed to the sea ice model and ocean model. After finishing one-step integration, sea ice model will transfer ice concentration, ice velocity, ice temperature and other variables to the coupler, and ocean model will transfer sea surface temperature, water velocity and salinity to the coupler. The next step is calculation of the flux again. During the calculation of ocean model, if fragile ice forms in ocean, the relevant variables in sea ice model and ocean model need to be modified synchronously, to make sure sea water temperature is kept at the freezing point. During the simulation, there are no ice fields restoring.

3. Simulation of the seasonal evolution of sea ice during the winters of 1997-2009

The ice-ocean coupled model was used to simulate sea ice evolution in the Bohai Sea and North Yellow Sea during the winters of 1997-2009. Simulation begins on October 15th every year. The spin-up time of coupled simulation is generally about 30 days. To determine the appropriate spin-up time, a series of ocean model sensitivity experiments have been done. At the same configuration, the ocean model are run under several different conditions including 1) no wind no tide, 2)with wind no tide 3)no wind with tide 4) with wind and tide. Results of sensitivity experiments in the Bohai Sea and North Yellow Sea show that 30 days are needed for the model to achieve stability in the case of no wind and no tide condition. However, it can achieve stability in several days with the influence of wind and tide. In actual simulation, spin-up time depends mainly on whether the simulated or forecasted surface temperature is consistent with the air and sea ice conditions at that time. Because of the difficulty of obtaining dynamically consistent initial field of sea surface temperature, the ocean model requires a separate run forced by meteorological conditions before it is coupled with sea ice model in order to get a more reasonable initial field of sea surface temperature.

3.1 ice period

Table 2 shows the comparison of ice-freezing date, ice-ending date and ice period of sea ice between the simulated results and observations. It can be seen from the table that ice-freezing date of sea ice is averagely 1 day later than the observed data. The biggest difference of the simulated ice-freezing date with the data is 12 days in advance and 9 days in lag. The percentage of the ice-freezing date difference less than 1 week is up to 75%. The ice-ending date of sea ice is averagely 2 days earlier than the observed data. The earliest ice-ending date is 9 days in advance, while the latest is 6 days in lag. The percentage of the ice-ending date error less than 1 week is higher than that of the ice-freezing

date, reaches 92%. The simulated ice period is averagely 4 days less than the observed data with the maximum error is 15 days shorter and 13 days longer than the analysis based on observed data. There are 50% of experimental years with the error of ice period not more than 1 week. In general, the simulated results of ice-freezing date, ice-ending date and ice period are very close to observations from the marine stations. The ice-ocean coupled reproduces the seasonal evolution of sea ice reasonably.

Table.2 Comparison of sea ice period between simulated results and observed analysis

Years	Ice-freezing date			Ice-ending date			Ice period(d)		
	Actual	Calculation	Error	Actual	Calculation	Error	Actual	Calculation	Error
1997-1998	1997.12.23	12.11	-12	1998.2.17	2.18	1	57	70	13
1998-1999	1998.12.05	12.02	-3	1999.2.18	2.16	-2	76	77	1
1999-2000	1999.12.18	12.19	-1	2000.2.24	3.02	6	69	74	5
2000-2001	2000.12.13	12.12	-1	2001.3.12	3.12	0	90	91	1
2001-2002	2001.12.07	12.15	8	2002.2.22	2.21	-1	78	69	-9
2002-2003	2002.12.08	12.08	0	2003.2.25	2.23	-2	60	58	-2
2003-2004	2003.12.06	12.12	6	2004.2.24	2.19	-5	80	69	-11
2004-2005	2004.12.20	12.20	0	2005.3.14	3.14	0	80	80	0
2005-2006	2005.12.06	12.10	4	2006.3.13	3.04	-9	98	85	-13
2006-2007	2006.12.17	12.28	1	2007.2.16	2.11	-5	62	47	-15
2007-2008	2007.12.29	12.31	2	2008.2.29	2.29	0	63	61	-2
2008-2009	2008.12.13	12.22	9	2009.3.06	3.03	-3	84	72	-12
Average error	1.08			-1.67			-3.67		
Max error	-12/9			-9/6			-15/13		
mean square deviation	5.58			3.72			8.44		

As for the relatively large differences of ice periods for some winters, we think the possible reason is that we use the same initial 3-d climatologically oceanic fields for ocean temperature and salinity in the POM model, but the actual 3-d oceanic fields may have some obvious differences during different winters. Further work should consider the real 3-d oceanic fields and make data assimilation to improve simulation accuracy.

3.2 The seasonal evolution of ice extent and ice area

Table 3 shows the comparison of the date of maximum sea ice coverage between simulated results and observed analysis from the winter of 1997/1998 to 2008/2009. It can be seen from the table that the average error of maximum ice coverage date is 2.33 days later than the observed data. The maximum error is 3 days early and 9 days later than the analysis based on observed data. The percentage of the maximum sea ice coverage date difference less than 1 week is up to 83%.

Table.3 Comparison of the date of maximum sea ice coverage between simulated results and observed analysis

Years	The date of maximum sea ice coverage		
	Actual	Calculation	Error
1997-1998	1998.1.31	1.28	-3
1998-1999	1999.1.12	1.12	0
1999-2000	2000.2.8	2.16	8
2000-2001	2001.2.16	2.16	0
2001-2002	2002.1.17	1.17	0
2002-2003	2003.2.5	2.11	6
2003-2004	2004.1.25	1.30	5
2004-2005	2005.2.25	2.26	1
2005-2006	2006.2.8	2.8	0
2006-2007	2007.1.24	1.28	4
2007-2008	2008.2.6	2.15	9
2008-2009	2009.2.3	2.1	-2
Average error	2.33		
Max error	-3/9		
mean square deviation	3.77		

Table 4 shows the comparison of the date of maximum sea ice extent of Liaodong Bay between simulated results and observed analysis from the winter of 1997/1998 to 2008/2009. It can be seen from the table that the average error of maximum ice extent is 7 nm smaller than the observed data. The maximum error is 20 nm less and 14 nm more than the analysis based on observed data.

Table.4 Comparison of maximum sea ice extent of Liaodong Bay between simulated results and observed analysis

Years	Maximum sea ice extent of Liaodong Bay (nm)		
	Actual	Calculation	Error
1997-1998	72	56	-16
1998-1999	58	38	-20
1999-2000	78	80	2
2000-2001	115	99	-16
2001-2002	48	36	-12
2002-2003	58	72	14
2003-2004	61	53	-8
2004-2005	76	90	14
2005-2006	77	74	-3
2006-2007	48	35	-13
2007-2008	66	55	-11
2008-2009	65	50	-15
Average error	-7		
Max error	-20/14		
mean square deviation	11		

Here we define ice extent as the distance between sea ice edge and coast along the central axis of the bay (shown as Fig. 1). Taking winter of 2005-2006 as an example, Figure 3a and 3b give daily variations of sea ice extent and ice area during the whole winter.

Figure 3a shows that sea ice formed at the end of 2005 and it had a rapid development during the ice freezing period. The severe period of sea ice is during late January and early February, with the simulated sea ice edge 74 nm (nautical mile) away from the top of the Liaodong Bay. This value is very close to the analysis from satellite image (78 nm). It also shows that the model could catch the process of sea ice rapid melting and the later freezing again in mid-February, as well as the retreating in early March. The simulated ice-ending date is earlier than the observed analysis, while the former is March 4, 2006, and the later

is March 13, 2006. Basically, the simulated evolution of sea ice extent has a consistent trend with observed situation. However, the simulated sea ice extent has a faster withdrawal than the observed situation during ice freezing period, ice developing period, and especially ice melting period. The reason may be related to the deviation of model input atmospheric forcing field as well as to the deficiency of sea ice model in the feedback mechanism of ice melting process. Further study is needed to solve this problem.

Sea ice area is defined as the sum of ice concentration in each grid of the study region. The simulated sea ice area (shown in Fig. 3b) is consistent with the developing process of the observed analysis from satellite remote sensing imageries. For ice area, the match in variation phase between simulation and observation is similar to that of the ice extent. However, the value is smaller in the majority of the ice period, except in late December and early January when the simulation of the ice area is larger than the observation. It can also be noticed that just the same as simulated ice extent, sea ice area decreased faster than the observation, causing significantly smaller ice area during the melting period.

As a whole, the simulation of sea ice extent and coverage reflects the characteristics of seasonal sea ice evolution, however, during the melting period of sea ice, simulated sea ice melts much faster than real conditions.

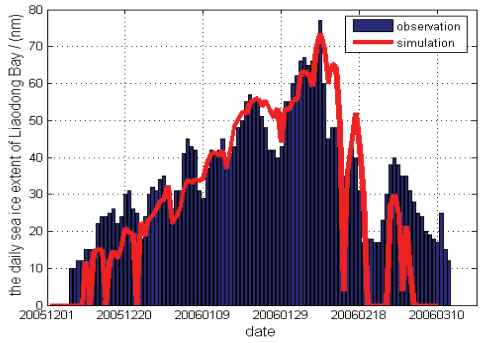

Fig.3a Simulated and observed daily ice extent in winter of 2005/2006

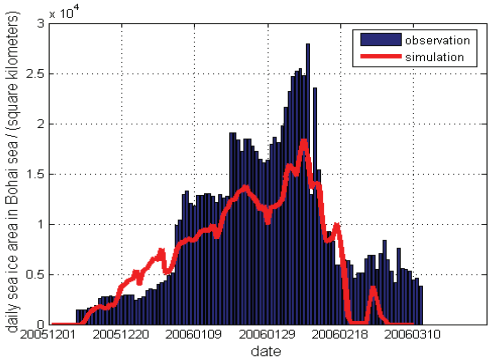

Fig.3b Simulated and observed daily ice area in winter of 2005/2006

3.3 Distribution of sea ice thickness and ice concentration

The simulated distribution of sea ice thickness and concentration also has been analyzed. Totally, simulated sea ice thickness and concentration in the Bohai Sea and North Yellow Sea can represent the basic characteristics of sea ice distribution.

Taking sea ice condition in the winter of 1999/2000 as an example, which was relatively severe and defined as "year of heavier ice". Figure 4 shows simulated sea ice thickness and ice concentration distribution during the most severe period of sea ice on February 3, 2000.

The most serious ice conditions appeared in Liaodong Bay in area of the Bohai Sea and North Yellow Sea. The simulated sea ice covered most area of Liaodong Bay. This is consistent with the NOAA's satellite remote sensing imagery (Figure 5). In winter, prevailing winds in Liaodong Bay are in northwest, north and northeast direction. Affected by tidal, sea water basically move to and fro along the central axis of the Liaodong Bay. Driven by the combined effects of wind and current, sea ice commonly drifts towards east and south. This causes the situation that sea ice in the east is thicker and it is thinner in the west of the bay. For the ice concentration, it is higher in central and eastern areas in the bay, while lower in the western and the top the bay. The model results well reproduced this sea ice concentration and thickness distribution in general. But the defect is that the ice thickness difference between the east area and the west area near the coast is significantly larger than that of satellite remote sensing data analysis. This is due to the model has an excessive accumulation of sea ice in east coast of the Liaodong Bay. Possibly, the value of sea ice compressive strength or the ice thickness distribution is not suitable for this domain. In addition, sea ice was not reproduced in the Fuzhou Gulf, a region southeast of Liaodong Bay.

Simulated sea ice concentration in the Bohai Bay, Laizhou Bay and North Yellow Sea can represent the basic characteristics of sea ice distribution with a higher concentration and thicker thickness in shallow waters near shore, while the value of simulated sea ice concentration is generally lower and ice thickness is thinner in these three bays. The future work should be to verify the water depth and the salinity fields of these three domains.

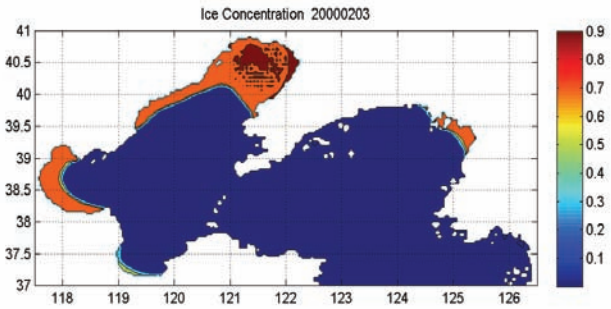

Fig.4a Simulated sea ice concentration (Feb.3, 2000)

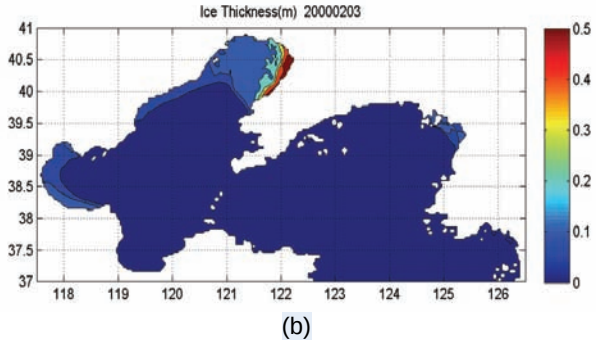

Fig.4b Simulated sea ice thickness(Feb.3, 2000）

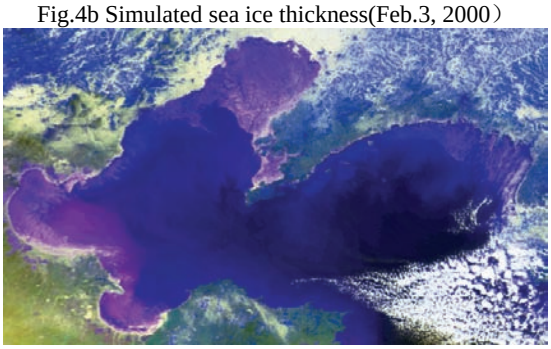

Fig.5 Remote sensing sea ice map from NOAA (Feb.3, 2000)

CONCLUSIONS AND DISCUSSIONS

In this paper, a brief introduction has been described for the ice-ocean coupled model in the Bohai Sea and North Yellow Sea. By using this coupled model and the regional atmospheric reanalysis data, numerical seasonal simulation and analysis of sea ice evolutions were undertaken for the winters from 1997/1998 to 2008/2009 in the Bohai Sea and North Yellow Sea. From the results of continuous simulations, it can be drawn that this ice-ocean coupled model can reproduce the seasonal sea ice evolutions well. Some results can be summarized as follows.

1）In general, the development of simulated sea ice conditions are consistent with the actual evolution processes, and the simulations of the ice-freezing date, ice-ending date and ice periods agree reasonably well with observations, and some are even identical to field data. The averaged errors of ice-freezing date, ice-ending date and ice period are only 1.08d, -1.67d and -3.67d respectively, and the maximum errors of those are -12d, -9d and -15d.

2) The simulation of sea ice extent and coverage reflects the characteristics of seasonal evolution of sea ice well, however, during ice-melting period, simulated sea ice melts much faster than reality. The averaged errors of maximum ice coverage date and maximum ice extent of Liaodong Bay are 2.33d and 7nm separately, and the maximum errors of those are 9d and 20nm.

3) Normally, the sea ice thickness of the west part in the Liaodong bay is less than that of the east part, which can be reproduced well by the ice-ocean coupled model. But the defect is that the ice thickness difference between the east area and the west area near the coast is significantly larger than that of satellite remote sensing data analysis.

4) Simulated sea ice concentration in the Bohai Bay, Laizhou Bay and North Yellow Sea can represent the basic characteristics of sea ice distribution, while the values of simulated sea ice concentration is generally lower and ice thickness is thinner.

To enhance simulation accuracy of ice period, ice extent and ice thickness, some further work should be done to this ice-ocean coupled model: a) To verify the water depth of the Bohai Bay, Laizhou Bay and North Yellow Sea and to get the real 3-d oceanic fields of oceanic temperature and salinity and take data assimilation for model initial fields. b) To check the meteorological field errors or feedback mechanisms of melting process in the model. c) To verify if the value of sea ice compressive strength and the ice thickness distribution are suitable.

ACKNOWLEDGEMENTS

We would like to thank the anonymous reviewers for their helpful suggestions. This research was supported by Project 908-02-03-06 and Marine Community Project (200805009 and 201105016).

REFERENCES

Bai S., Liu Q., Li H. and Wu H. (1998). *Sea Ice Disaster in 1969*, China Ocean Press, Beijing, 115-122 pp. (In Chinese)

Bai S., Wu H. (1998). "Numerical Sea Ice Forecast for the Bohai Sea," *Acta Meteorologica Sinica*, Vol 56, No 2, pp 139-152. (In Chinese)

Blumberg, A.F., Mellor, G.L. (1987). *A Description of a three-dimensional Coastal Ocean Circulation Model*, American Geophysical Union, 208 pp.

Colony R, Rothrock D A (1980). *A Perspective of the Time-dependent Pesponse of the AIDJEX Model*, University of Washington Press, 124-133 pp.

Editorial Board of Ocean Atlas (1993). *Atlas of the Bohai Sea, Yellow Sea And East China Sea (hydrology)*, China Ocean Press, Beijing, 524 pp. (In Chinese)

Hibler W. D. (1979). "A Dynamic Thermodynamic Sea Ice Model," *J Phys Oceanogr*, Vol 9, pp 815-846.

Hibler W. D. (1980). "Modeling a Variable Thickness Sea Ice Cover," *Mon Wea Rev*, Vol 108, pp 1943-1973.

Liu Q., Huang J. (2000). "Global Simulation of Sea Ice with a Coupled Ice-ocean Model," *Earth Science Frontiers*, Vol 7, supplement, pp 219-230. (In Chinese)

Liu Q., Bai S. (2004). "A Thermodynamic Coupling Scheme for Ice-ocean Coupled Model," *Acta Oceanologica Sinica*, Vol 26, No 6, pp 13-21. (In Chinese)

Liu Q., Zhang J. (2005). "Numerical Forecast for the 3-dimensional Sea Temperature and Current in the Bohai Sea", *Marine Forecasts*, Vol 22, supplement, pp 30-37. (In Chinese)

Mellor, G.L. and L.H. Kanthan (1989). "An Ice-ocean Coupled Model," *J. Geophys. Res.*, Vol 94, No C8, pp 10937-10954.

Su J., Wu H., Zhang Y., Liu Q. and Bai S. (2004). "A Coupled Ice-ocean Model for the Bohai Sea: I. Study on Model and Parameter," *Acta Oceanologica Sinica*, Vol 23, No 4, pp 597-608.

Su J., Wu H., Zhang Y., Bai S., and Liu Q. (2005). "A Coupled Ice-ocean Model for the Bohai Sea: II. Case Study," *Acta Oceanologica Sinica*, Vol 24, No 3, pp 54-67.

Thorndike, A. S., Rothrock, D. A., Maykut, C. A. and Colony, R. (1975). "The Thickness Distribution of Sea Ice," *J. Geophys. Res.* Vol 80, No 33, pp 4501-4513.

Wu H. (1991). "Mathematic Representations of Sea Ice Dynamic Thermodynamic Processes," *Oceanologia Et Limnologia Sinica*, Vol 22, No 4, pp 221-228. (In Chinese)

Wu H., Wang Z. (1992). *The Thermal Prosess of Sea Ice and It's Numerical Simulation*, Henan Science and Technology Press, 361-428 pp. (In Chinese)

Wu H., Bai S. (1995). *Sea Ice Rheology*, National Defense University Press, 40-49 pp. (In Chinese)

Wu H., Bai S. (1998). "Numerical Simulation for Dynamical Process of Sea Ice," *Acta Oceanologica Sinica*, Vol 25, No 3, pp 301-305.

Wang J., Liu Q. (2005). "A Coupled Ice-Ocean Model in the Pan-Arctic and North Atlantic Ocean: Simulation of Seasonal Cycles," *Journal of Oceanography*, Vol 61: pp 213-233.

Wang R. (1982). "The Relation between Air-sea Heat Exchange and Sea Ice Growth and Regression in the Bohai Sea," Marine Environmental Science, No 2, pp 74-79. (In Chinese)

Wang R., Liu X. (1984). "The Numerical Simulation of Sea Ice in the Bohai Sea," *Acta Oceanologica Sinica*, Vol 6, No 5, pp 572-586. (In Chinese)

Wang R., Liu Q. (1994). "Numerical Simulation and Tests of Sea Ice Drift Process in the Bohai Sea," *Oceanologia Et Limnologia Sinica*, Vol 25, No 3, pp 301-305. (In Chinese)

Wang Z., Wu H. (1994). "Sea Ice Thermal Processes and Simulation of their Coupling with the Dynamic Process," *Oceanologia Et Limnologia Sinica*, Vol 25, No 4, pp 408-415. (In Chinese)

Yao T., Tang C. L., Peterson I. K. (2000). "Modeling the Seasonal Variation of Sea Ice in the Labrador Sea with a Coupled Multicategory Ice Model," *J Geophys Res*, Vol 105, No C1, pp 1153-1165.

Yang S., Bai S. (1991). "Research on the Application of Short-term Numerical Sea Ice Forecast," *Marine Forecasts*, Vol 8, No 4, pp 1-11. (In Chinese)

Zhang Q., Li B., Bai S. (2008). "A Rare Seen Sea Ice Disaster and Formation Cause Analysis at the Fisherman Village of LongGang of the Huludao in 1/2007," *Marine Forecasts*, Vol 25, No 1, pp 20-24. (In Chinese)

Zhang F. (1986). *Sea Ice in China*, China Ocean Press, Beijing, 165 pp. (In Chinese)

Zhang X., Zhao Q. (2000). *Ocean Circulation-ice Model and Air-sea Coupling Research Progress*, Meteorological Press, 161-169 pp. (In Chinese)